Significant increase of summertime ozone at Mt. Tai in Central Eastern China: 2003-2015

Lei Sun[1], Likun Xue[1*], Tao Wang[2,1], Jian Gao[3], Aijun Ding[4], Owen R. Cooper[5,6], Pengju Xu[7], Zhe Wang[2], Xinfeng Wang[1], Liang Wen[1], Yanhong Zhu[1], Tianshu Chen[1], Lingxiao Yang[1,8], Yan Wang[8], Jianmin Chen[1,8], Wenxing Wang[1]

[1] Environment Research Institute, Shandong University, Ji'nan, Shandong, China

[2] Department of Civil and Environmental Engineering, Hong Kong Polytechnic University, Hong Kong, China

[3] Chinese Research Academy of Environmental Sciences, Beijing, China

[4] Institute for Climate and Global Change Research and School of Atmospheric Sciences, Nanjing University, Nanjing, Jiangsu, China

[5] Cooperative Institute for Research in Environmental Sciences, University of Colorado, Boulder, Colorado, United States

[6] NOAA Earth System Research Laboratory, Boulder, Colorado, United States

[7] School of Geography and Environment, Shandong Normal University, Ji'nan, Shandong, China

[8] School of Environmental Science and Engineering, Shandong University, Ji'nan, Shandong, China

*To whom correspondence should be addressed: Likun Xue: xuelikun@sdu.edu.cn

Abstract.

Tropospheric ozone (O_3) is a trace gas playing key roles in atmospheric chemistry, air quality and climate change. In contrast to North America and Europe, China has limited long-term records of surface O_3 that can be used to establish trends. In this study, we compiled the available observations of O_3 at Mt. Tai – the highest mountain over the North China Plain (NCP), and analyzed their seasonal and diurnal behavior as well as the trends over 2003–2015. The summertime climatological air mass

transport pattern was established by back trajectory calculation and a subsequent cluster analysis. A significant increase of surface O_3 ($p < 0.01$) in the summertime from 2003 to 2015 was derived from a linear regression analysis, with increasing rates of 1.7 ppbv yr^{-1} for June and 2.1 ppbv yr^{-1} for the July–August period. Analysis of satellite trace gas retrievals indicates that the O_3 increase was mainly

5   due to the increased emissions of O_3 precursors, in particular volatile organic compounds (VOCs). An important finding is that the emissions of nitrogen oxides (NO_x) have diminished since 2011, but the increase of VOCs appears to have enhanced the ozone production efficiency and contributed to the observed O_3 increase in northern China. This study provides direct evidence that controlling NO_x alone, in the absence of VOC controls, is not sufficient to reduce regional O_3 levels in North China. In addition,

10   the ozone observations at this regionally representative mountain site are ideal for evaluating global and regional scale chemical transport models.

1. Introduction

Ozone (O_3) in the troposphere is a trace gas of great importance for climate and air quality. It is the principal precursor of the hydroxyl radical (OH) which plays a central role in atmospheric chemistry

15   (Seinfeld and Pandis, 2006), and the third most important greenhouse gas contributing to the warming of the Earth (IPCC, 2013). At ground level, high levels of O_3 have adverse effects on human health and ecosystem productivity (National Research Council, 1991; Monks et al., 2015). In the troposphere, the ambient O_3 burden is the product of the flux from the stratosphere (Stohl et al., 2003), dry deposition, and net photochemical production involving the reactions of nitrogen oxides (NO_x) with carbon

20   monoxide (CO) and volatile organic compounds (VOCs) in the presence of sunlight (Crutzen, 1973; Ma et al., 2002). Increases in anthropogenic emissions of ozone precursors have driven changes in the tropospheric O_3 abundances, both globally and regionally (Cooper et al., 2014; Monks et al., 2015; The Royal Society, 2008). Conversely, the changing tropospheric O_3 may also pose significant feedbacks to the environment and climate (e.g., Shindell et al, 2012; Stevenson et al, 2013). Therefore, the long-term

25   changes (or trends) of tropospheric O_3 has long been a topic of great interest in the atmospheric sciences.

Atmospheric
Chemistry
and Physics
Discussions

Open Access

EGU

Since the 1970s, long-term measurements of surface O_3 (and O_3 precursors) have been increasingly carried out worldwide, mostly in North America and Europe (Cooper et al., 2014; and references therein). The existing knowledge of tropospheric O_3 trends has been recently reviewed (Cooper et al., 2014; Monks et al., 2015; UNEP, 2011). Overall, upward trends have been recorded around the world since the 1970s, but trends over the past two decades have varied regionally. In Europe, the surface O_3 in rural or remote areas, usually regarded as the regional background O_3, rose until the year 2000 but has since leveled off or decreased (Oltmans et al., 2013; Parrish et al., 2012). In the eastern US, summertime O_3 at most rural and urban stations has decreased over 1990–2010 (Cooper et al., 2014; Lefohn et al., 2010). In the western US, extreme ozone events have decreased in urban areas but rural ozone has either remained steady or even increased during springtime (Cooper et al., 2012; Oltmans et al., 2013; Parrish et al., 2012). In contrast, the limited measurements in East Asia have shown significant increasing trends in the regional background O_3 since the 1990s (Cooper et al., 2014; and references therein).

In comparison with North America and Europe, investigations of long-term O_3 trends are scarce in China, where rapid urbanization and industrialization has occurred over the past three decades. Although significant increasing trends of surface O_3 have been derived from long-term air quality monitoring or series of short-term measurements at urban and suburban sites in Beijing (Tang et al., 2009; Zhang et al., 2014), Hong Kong (Xue et al., 2014), and Taiwan (Lin et al., 2010), long-term observations covering more than ten years in rural or remote areas (indicative of the regional background O_3 trend) remain very limited (Cooper et al., 2014). Wang et al. (2009) reported the first long-term continuous observations of Chinese surface O_3 at a regional background site in southern China (Hok Tsui), and indicated an average increase of 0.58 ppbv yr^{-1} during 1994–2007. Xu et al. (2015) recently reported another continuous ozone record (1994–2013) at Mt. Waliguan, a Global Atmospheric Watch station in western China, and also found significant positive trends with 0.15–0.27 ppbv yr^{-1} for daytime O_3 and 0.13–0.29 ppbv yr^{-1} for nighttime O_3. Based on the MOZAIC commercial aircraft measurements, Ding et al. (2008) derived an ozone increase of ~2% per year from 1995 to 2005 for the lower troposphere above Beijing by analyzing the difference between observations from

Atmospheric
Chemistry
and Physics
Discussions

1995–2000 and 2000–2005. Despite the valuable information obtained from the abovementioned efforts, additional studies are required to improve our understanding of tropospheric O_3 trends across the rapidly developing China.

In recent years, China has phased in a series of stringent air quality control measures. Following the

5   successful reductions in sulfur dioxide (SO_2) emissions in 2006 (Lu et al., 2010), China has recently launched a national programme to reduce NO_x emissions during its "Twelfth Five-Year Plan" (2011–2015) (China State Council, 2011). However, to our knowledge, few controls have been placed on VOC emissions in China. Rather, anthropogenic VOC emissions have continued to increase (Bo et al., 2008; Wang et al., 2014). Therefore, it is of great interest and critical importance to evaluate the

10   effect of the current control policy (i.e., controlling NO_x with little action for VOCs) on regional O_3 and other secondary air pollution problems in China.

Mt. Tai (36.25 °N, 117.10 °E; 1534 m above sea level (a.s.l.)) is the highest mountain in the center of the North China Plain (NCP; see Fig. 1) – a fast developing region facing severe air pollution. During daytime, its summit is well within the planetary boundary layer (PBL), and the site is therefore

15   regionally representative of the NCP region (Kanaya et al., 2013). Since 2003, several field measurement campaigns have been conducted at the site, with surface O_3 of major interest. In this paper, we analyze all available ozone and ozone precursor observations at Mt. Tai to understand the summertime O_3 characteristics, including trends. In the following sections, we first present the seasonal and diurnal ozone variations followed by the climatological air mass transport pattern in summer; we

20   then derive the O_3 trend (or systematic change) during 2003–2015 using linear regression; we finally elucidate the key factors affecting the O_3 trends by examining satellite and in-situ observed trace gas data. Our analysis demonstrates a significant increase of summertime surface ozone at this important regional site in northern China, and indicates the urgent need of VOC control in China to reduce regional ozone pollution.

25   **2. Observational data set**

The observations analyzed in the present study are summarized in Table 1. It comprises several sets

Atmospheric
Chemistry
and Physics
Discussions

of field observations from different periods. The earliest ozone measurements at Mt. Tai were made from July–November 2003 (Gao et al., 2005), and the longest observations lasted for three years from June 2006 to June 2009 (despite a data gap in January–February 2007 owing to instrument maintenance). In recent years, we conducted intensive measurements at Mt. Tai during summer, i.e.

5 June–August, of 2014 and 2015. In addition, another set of 3-year measurements was carried out from March 2004 to May 2007, as an international joint effort between Japanese and Chinese scientists (Kanaya et al., 2013); monthly average O_3 data are taken from this work. As most of the measurements are available for the period of June–August each year, we focus on the summertime O_3 in this study.

Two study sites have been used for field observations at Mt. Tai. One was the Mt. Tai

10 Meteorological Observatory (Site 1) at the summit with an altitude of 1534 m a.s.l., and the other was in a hotel (Site 2) that is ~1 km to the northwest of Site 1 and slightly lower (1465 m a.s.l.; see *Fig. S1* for the site locations). Such elevations position these sites either within the PBL in the afternoon in summer, or in the free troposphere during the night. Although Mt. Tai is a famous tourism spot, both sites are located in the less frequently visited zones. Hence the impact of local anthropogenic emission should be

15 small, and the data collected are believed to be regionally representative. Details of these sites have been described elsewhere (Site 1: Gao et al., 2005; Kanaya et al., 2013; Site 2: Guo et al., 2012; Shen et al., 2012). For our data set, most of the measurements were taken at Site 1, and only the intensive campaign in 2014 took place at Site 2.

All measurements were implemented using standard techniques, which were detailed in the

20 previous publications (e.g., Gao et al., 2005; Xue et al., 2011). Briefly, O_3 was measured using a commercial ultraviolet photometric instrument (*Thermo Environment Instruments (TEI), Model 49C*) with a detection limit of 2 ppbv and a precision of 2 ppbv. CO was monitored with a gas filter correlation, non-dispersive infrared analyzer (*Teledyne Advanced Pollution Instrumentation, Model 300E*), with automatic zeroing every two hours. This technique has a detection limit of 30 ppbv and a

25 precision of 1% for a level of 500 ppbv. NO and NO_2* were measured by a chemiluminescence analyzer equipped with an internal MoO catalytic converter (*TEI, Model 42C*), with a detection limit of 0.4 ppbv and precision of 0.4 ppbv. Inter-comparison with a highly selective photolytic NO_2 detection

Atmospheric
Chemistry
and Physics
Discussions

Open Access

EGU

approach indicated that the NO_2* measured with MoO conversion significantly overestimated NO_2 (i.e.,

up to 130% in afternoon hours), and NO_2* actually represented a major fraction (60%–80%) of NO_y at

Mt. Tai (Xu et al., 2013). During the measurements, the O_3 analyzer was calibrated routinely (i.e.,

quarterly for the 3-year observations in 2006–2009, and before and after the other campaigns) by an

5 ozone primary standard (*TEI, Model 49PS*). For CO and NO_x*, zero and span calibrations were

performed weekly during 2006–2009 and every three days during the intensive campaigns.

Meteorological data including temperature, relative humidity (RH), and wind vectors were obtained

from the Mt. Tai Meteorological Observatory, where Site 1 is located.

It is noteworthy that some portion of this long-term data set has been reported previously. Gao et al.

10 (2005) analyzed the measurements of O_3 and CO from July–November 2003 and examined their diurnal

variations and relations to backward trajectories. Kanaya et al. (2013) reported the observations in

2004–2007 and examined the processes influencing the seasonal variations and regional pollution

episode. The major objective of the present study is to compile all of the available O_3-related

observations at Mt. Tai and to establish the trend (or systematic change), if any, of ambient O_3 levels in

15 the past decade at this unique site, regionally representative of the NCP.

3. Results and discussion

3.1. Seasonal and diurnal variations from more recent data

Figure 2 depicts the seasonal variation of surface O_3 at Mt. Tai derived from the more recent

year-round observations from 2006–2009. Overall, O_3 shows higher levels in the warm season, i.e.

20 April–October, compared to the cold season, i.e. November–March, with two peaks in June and October.

In addition to the high temperatures and intense solar radiation (especially in June), biomass burning is

believed to be another factor shaping the O_3 maximums in June and October, both of which are major

harvest seasons of wheat and corn in northern China. The significant impacts of biomass burning on air

quality at Mt. Tai have been evaluated by Yamaji et al. (2010) and Suthawaree et al. (2010). Modeling

25 and data analysis studies usually averaged the O_3 levels in June, July and August (JJA) to represent the

overall summertime condition (e.g., Lin et al., 2008 and 2009). For the Mt. Tai case, however, it is

noticeable that the O_3 concentrations in July and August were substantially lower than those in June. This is attributable to the more humid weather and greater precipitation in July and August in this region (see Table 2 for the RH condition). Inspection of meteorological conditions day by day also indicated a frequency of cloudy days (i.e., with RH ≥ 95%) of ~25% in June and of ~51% during July–August. In

5 the following analyses, therefore, we assess the ozone characteristics separately for June and July–August.

Shown in the upper panel of Fig. 2 is the frequency of the maximum daily 8-hour average O_3 mixing ratios (MDA8 O_3) exceeding the national ambient air quality standard (i.e., 75 ppbv; Class II). Although located in a relatively remote mountain-top area, the observed O_3 pollution at Mt. Tai was

10 rather serious in the warm season, with frequencies of the O_3-exceedence days of over 45% throughout April–October. In particular, the occurrence of O_3-exceedence days was as high as 89% in June. These results demonstrate the severe O_3 pollution situation across the North China Plain.

Figure 3 illustrates the well-defined diurnal variations of surface O_3 with a trough in the early morning and a broad peak lasting from afternoon to early evening, which is commonly observed at

15 polluted rural sites. As the summit of Mt. Tai is well above the planetary boundary layer at nighttime, the O_3 concentrations during the latter part of the night (e.g., 2:00–5:00 LT) are usually considered to represent the regional background O_3. Comparing the diurnal profiles in June and July–August clearly reveals the significantly higher regional background O_3 in June (with a mean difference of ~17 ppbv). On the other hand, the daytime O_3 build-up, defined as the increase in O_3 concentrations from the

20 early-morning minimum to the late-afternoon maximum, may reflect the potential of regional O_3 formation. For the Mt. Tai case, the average daytime O_3 build-up was 22 ppbv in June and 15 ppbv in July–August, indicating the stronger photochemical ozone production in June. Hence, the more intense photochemistry and higher regional background bring about the more serious O_3 pollution in June at Mt. Tai.

25 Another remarkable feature of surface O_3 at Mt. Tai is the relatively high nighttime levels, with average concentrations of 75–85 ppbv in June and 60–70 ppbv during July–August. This should be the

composite result of the residual O_3 produced in the preceding afternoon in the boundary layer, less O_3

loss from NO titration, and long-range transport of processed regional plumes. The latter was evidenced

by the coincident evening NO_2^* maximums and low NO levels, as shown in Fig. 4. Inspection of the

time series day by day also reveals the frequent transport of photochemically aged air masses containing

5   elevated concentrations of O_3 (over 100 ppbv), CO and NO_2^* to the study site during the late evening

(figures not shown). Similarly, the MOZAIC aircraft measurements have also found ~60 ppbv on

average of O_3 at around 1500 m a.s.l. over Beijing at 5:00–6:00 LT in summer (i.e., May–July; Ding et

al., 2008), which is comparable to what we observed at Mt. Tai. These results imply the existence of the

O_3-laden air in the nocturnal residual layer over the NCP region. Moreover, Ding et al. (2008) also

10   showed in their Figure 11 that the O_3 enhancement extended from the surface up to about 2 km, further

evidence that during the daytime Mt. Tai should be within the boundary layer and is sampling at a

vertical level where ozone enhancements are expected.

3.2. Impact of long-range transport

Long-range transport associated with synoptic weather and large-scale circulations is an important

15   factor for the variation of ozone in rural areas (Wang et al., 2009; Ding et al., 2013; Zhang et al., 2016).

To elucidate the history of air masses sampled at Mt. Tai, we analyzed the summertime climatological

air mass transport pattern during 2003–2015 with the aid of cluster analysis of back trajectories. The

detailed methodology has been documented by Wang et al. (2009) and Xue et al. (2011).

Three-dimensional 72-hour back trajectories were computed four times a day (i.e., 2:00, 8:00, 14:00 and

20   20:00 LT) for June–August with the Hybrid Single-Particle Lagrangian Integrated Trajectory model

(HYSPLIT, v4.9; Draxler et al. 2009), with an endpoint of 300 m above ground level exactly over Mt.

Tai. All the trajectories were then categorized into a small number of major groups with the HYSPLIT

built-in cluster analysis approach.

A total of five air mass types were extracted for the summer period, with four identified for June

25   and July–August respectively. These air mass types are named according to the regions they traversed,

and are described as follows: "Marine and East China" (M&EC) – air masses from the east passing over

the ocean and polluted central eastern China; "Northeast China" (NEC) – air masses from the north passing over Northeast China; "Central China" (CC) – air masses from the south moving slowly over central China; "Southeast China" (SEC) – air masses from the south moving fast from southeast China; "Mongolia and North China" (M&NC) – air masses from the northwest passing over Mongolia and central northern China.

The above identified major types of air masses are presented in Fig. 5. In June, M&EC was most frequent (57%), followed by CC (26%), NEC (9%) and M&NC (8%; only identified in June). During the July–August period, the most frequent air mass type was still M&EC (36%), then CC (29%) and NEC (29%), with a minor fraction of SEC (6%; only identified in July–August). Overall, the transport patterns in June and July–August are quite similar, and it is evident that southerly and easterly pathways dominated the air mass transport to Mt. Tai in summer. Such patterns are believed to be driven by the summer Asian monsoon (Ding et al., 2008).

The chemical signatures of the different air masses were also inspected and summarized in Table 3. The air masses of M&EC, CC and NEC, which passed over several polluted regions of eastern China, contained higher abundances of O_3 (with averages of 89–94 ppbv in June and 64–77 ppbv in July–August), CO and NO_2*. In comparison, the more aged air masses of M&NC and SEC showed relatively lower concentrations of O_3 (78 ± 21 ppbv for M&NC in June and 58 ± 17 ppbv for SEC in July–August) and its precursors (except for NO_2* in the SEC air mass). Therefore, the regions with the greatest influence on O_3 at Mt. Tai in summer are primarily located in the southern and eastern parts of central eastern China.

3.3. Ozone Trend

Figure 6 presents the monthly average hourly O_3 and MDA8 O_3 mixing ratios in June and July–August whenever available from 2003–2015 at Mt. Tai. The least square linear regression analysis reveals the significant increase of surface O_3 at Mt. Tai since 2003. Monthly mean O_3 values based on hourly data increased at rates of 1.7 ± 1.0 ppbv yr^{-1} ($\pm95\%$ confidence intervals) in June and 2.1 ± 0.9 ppbv yr^{-1} in July–August, and the increases were statistically significant ($p < 0.01$). For the monthly

means based on MDA8 O_3, the fewer available data points (as we only have monthly average data during 2004–2005 from Kanaya et al., 2013) likely reduced the significance of the trend in June, with a positive by statistically insignificant increase (rate = 1.4 ± 1.9 ppbv yr^{-1}; $p = 0.12$). However the site had a significant positive trend in July–August (rate = 2.2 ± 1.2 ppbv yr^{-1}; $p < 0.01$). Therefore we conclude

5   that summertime surface O_3 levels at Mt. Tai have increased over the period 2003–2015.

Given the fact that Mt. Tai is above the PBL at night when there is no photochemistry, the ambient O_3 levels before dawn (e.g., 2:00–5:00 LT) are representative of the regional background O_3. The diurnal variation in Fig. 3 shows a slight but steady decrease in O_3 concentrations overnight, which should arise from dry deposition. It was assumed that dry deposition was essentially the same every

10   year and did not affect the derived trends. Figure 7 shows the monthly averaged late-night O_3 mixing ratios in June and July–August available from 2003–2015 at Mt. Tai. Again, positive trends were found. The rate of increase was quantified at 1.9 ± 1.8 ppbv yr^{-1} ($p = 0.04$, significant) in June and 1.1 ± 1.2 ppbv yr^{-1} ($p = 0.06$, insignificant) during July–August. The increase of regional background likely explains the observed O_3 rise at Mt. Tai in June and also accounts for the majority of the increase during

15   July–August. These results indicate the significant increase of surface O_3 in summer on the regional scale across northern China.

Table 4 compares the surface and lower tropospheric ozone trends available in East Asia in recent decades. Two aspects are particularly noteworthy from this comparison. First, most studies have deduced significant positive trends demonstrating the broad increase of tropospheric O_3 over East Asia,

20   especially in China. This pattern is distinct from that found in Europe and the eastern U.S., where O_3 levels have begun to decrease or level off since the 1990s or 2000s (e.g., Cooper et al., 2014; Lefohn et al., 2010; Oltmans et al., 2013; Parrish et al., 2012). The ozone increase in East Asia is expected due to the rapid economic growth and increasing anthropogenic emissions of O_3 precursors in the past three decades (*e.g.,* Ohara et al., 2007). Second, the magnitude of O_3 increase is quite heterogeneous in

25   different regions and the fastest rise was found in the NCP. For example, the rates of O_3 increase were in the range of 0.54-0.58 ppbv yr^{-1} in Hong Kong (1994-2007, Wang et al., 2009; 2002-2013, Xue et al., 2014), 0.54 ppbv yr^{-1} in Taiwan (1994-2007, Lin et al., 2010), 0.26-0.55 ppbv yr^{-1} over South Korea

Atmospheric
Chemistry
and Physics
Discussions

(1990-2010, Lee et al., 2013; 1999-2010, Seo et al., 2014), 0.22-0.37 ppbv yr^{-1} in major Japanese metropolitan areas (1990-2010; Akimoto et al., 2015), 0.64 ppbv yr^{-1} at Mt. Happo, Japan (1991-2011, summer scenario; Parrish et al., 2014), and 0.15 ppbv yr^{-1} at Mt. Waliguan, a GAW station in western China (1994-2013, summer scenario; Xu et al., 2015). According to the MOZAIC aircraft observations,

5   in comparison, Ding et al. (2008) have reported the PBL O_3 increases of ~1 ppbv yr^{-1} for the annual average and ~3 ppbv yr^{-1} for the summer afternoon peaks over the period of 1995-2005. Zhang et al. (2014) analyzed their field measurements at an urban site in Beijing during 2005-2011 and quantified an increasing rate of 2.6 ppbv yr^{-1} for the daytime average O_3 in summer. Comparable rates of O_3 increase (1.7-2.1 ppbv yr^{-1}) were determined in the present study from the measurements of longer time coverage

10   and at a more regionally representative mountain site, affirming the significant rise of surface O_3 levels over the NCP region. Furthermore, the magnitude of O_3 increase in the NCP region is also among the highest records currently reported in the world (Cooper et al., 2012 and 2014; Lin et al., 2014; Parrish et al., 2014).

3.4. Roles of meteorology and anthropogenic emissions

15   Meteorology and changes in anthropogenic emissions may affect tropospheric O_3 directly (Monks et al., 2015; Mao and Talbot, 2004). To further elucidate the factors which have driven the increase of surface O_3 at Mt. Tai, we examined the long-term variations in both meteorological condition and anthropogenic emissions of O_3 precursors during the past decade. Table 2 summarizes the summertime mean meteorological conditions including average temperature, RH, and prevailing wind direction

20   recorded at Mt. Tai over the period of 2003–2015. Though some variability is clearly shown, no systematic change was found with regard to the overall meteorological conditions. We also explored the air mass transport pattern deduced from cluster analysis of back trajectories (see Section 3.2) year by year over 2003–2015 (*Table S1*). Despite the quite large year-to-year variability, again, no systematic change in the air mass transport pattern was indicated during the target period. Although the impact of

25   meteorology on tropospheric ozone is very complex and might not be quantified by such a simple analysis, the significant increase of surface O_3 observed at Mt. Tai should not primarily arise from the change in meteorological conditions.

Atmospheric
Chemistry
and Physics

Discussions

We then analyzed the satellite retrievals of formaldehyde (HCHO) and NO_2 to track the variations

in the abundances of O_3 precursors (i.e., NO_x and VOCs) during the study period. HCHO was adopted

as an indicator of VOCs since it is a major oxidation product of VOCs and because of the availability of

satellite products. The satellite data were obtained from SCIAMACHY for 2003–2011 and GOME-2(B)

5   from 2013 onwards, with the Level-2 products taken from the TEMIS archive (Tropospheric Emission

Monitoring Internet Service; http://www.temis.nl/index.php). Considering the geographical

representativeness of Mt. Tai, a larger domain (32 °–38 ° N, 115 °–120 ° E; see *Fig. 5*) was selected to

process the regional mean satellite data. The monthly averaged HCHO and NO_2 column densities in

June and July–August from 2003–2015 are documented in Fig. 8. Significant positive trends are seen

10   for HCHO, with rates of $2.7\% \pm 2.2\%$ ($p = 0.02$) for June and $2.2\% \pm 1.4\%$ ($p < 0.01$) for July–August,

indicative of the strong increase of VOCs in this region. This result agrees with the emission inventory

estimates which showed significant increases of anthropogenic VOC emissions in China in the past

decades (Bo et al., 2008; Wang et al., 2014), and is consistent with the lack of nationwide VOC

controls.

15   What is more interesting is the two-phase variation of the NO_2 column, showing a significant

increase first from 2003 to 2011 (June: $4.8\% \pm 3.4\%$, $p = 0.01$; July–August: $7.7\% \pm 3.6\%$, $p < 0.01$)

and a decrease afterwards (see Fig. 8b). These satellite observations agree very well with the bottom-up

emission inventory estimates, which clearly showed a break point occurring in 2011 in the

anthropogenic NO_x emissions of China (see *Fig. S2*). China has just launched a national NO_x control

20   programme during its "Twelfth Five-Year Plan" (i.e., 2011–2015) (China State Council, 2011). The

strict control measures are very efficient and have resulted in an immediate reduction of NO_x emissions,

as affirmed by both emission inventories and satellite retrievals. Furthermore, the reduced levels of NO_x

in the most recent five years were also evidenced by our limited in-situ NO_x* measurements at Mt. Tai.

As shown in Fig. 9, the ambient NO_2* levels in 2014 and 2015 were indeed substantially lower than

25   those measured in the previous years before 2010.

From the above analyses, the O_3 increase between 2003 and 2011 is easy to understand in light of

Atmospheric
Chemistry
and Physics
Discussions

the consistent increase of both NO_x and VOCs. For the later period, i.e. after 2011, in comparison, opposite trends have taken place with NO_x decreasing but VOCs still increasing. The observed continuing O_3 rise suggests that the reduction of NO_x is not adequate to reduce the ambient O_3 levels, with a background of increasing VOCs. We then evaluated the ozone production efficiency (OPE) for

5   the air masses sampled at Mt. Tai. OPE is usually derived from the regression slope of the scatter plots of O_3 versus NO_z (Trainer et al., 1993), and is a useful metric to infer how efficient O_3 is produced per oxidation of unit of NO_x (e.g., Wang et al., 2010; Xue et al., 2011). As NO_y (and thus NO_z) is not routinely measured in the present study, NO_2* is used instead of NO_z to infer the OPE values. It should be reasonable considering that our measured NO_2* significantly overestimated true NO_2 and actually

10   contained a large fraction of NO_z, especially in the afternoon period when NO_z was at its maximum with NO_2 at the minimum (Xu et al., 2013). The scatter plots of O_3 versus NO_2* during the afternoon hours (i.e., 12:00–18:00 LT) available from 2006–2015 at Mt. Tai are presented in Fig. 10. The OPE values in 2014–2015 (i.e., 9.6-15.0) were significantly higher than those determined during 2006–2009 (i.e., 3.6-7.9). This demonstrates the greater ozone production efficiency in recent years with increasing

15   VOCs. These results indicate that although NO_x in China has been reduced since 2011, little action on VOC control has led to increased emissions of VOCs, which could make O_3 formation more efficient per unit of NO_x. As a consequence, ambient O_3 levels have been rising in northern China. We conclude that control of VOCs is urgently needed, in addition to the ongoing strict NO_x control, to mitigate regional O_3 pollution in China.

20   **4. Summary**

In the present study, we compiled all field observations of O_3 and O_3 precursors ever collected at Mt. Tai, the highest point of the NCP, and found a significant increase of surface O_3 in summertime over 2003–2015 at this regionally representative site. The rising O_3 levels are primarily attributable to the increasing anthropogenic emissions of O_3 precursors, especially VOCs. Since 2011, NO_x has been

25   reduced efficiently by a strict national control programme, as evidenced by emission inventory estimates, satellite remote sensing and field observations. At the same time, VOC emissions increased, which enhanced the O_3 production efficiency and resulted in an overall O_3 increase in northern China.

This study provides direct evidence that the current Chinese control programme, focusing on NO_x alone with little action for VOCs, is not sufficient for mitigating regional O_3 pollution, and calls on the implementation of VOC controls as soon as possible. Similar to the U.S., China phased in its air pollution control measures resulting in decreasing SO_2 emission after 2006 and NO_x emission after 2011.

5   It is foreseen that the national VOC control will be launched very soon. Thus, follow-up long-term measurements are required to evaluate the response of ambient O_3 to the upcoming VOC control and to provide observational constraints to evaluate global and regional chemical transport models.

Acknowledgements

References

Akimoto, H., Mori, Y., Sasaki, K., Nakanishi, H., Ohizumi, T., and Itano, Y.: Analysis of monitoring data of ground-level ozone in Japan for long-term trend during 1990-2010: Causes of temporal and spatial variation, *Atmos. Environ.,* 102, 302-310, 2015.

20   Bo, Y., Cai, H., and Xie, S. D.: Spatial and temporal variation of historical anthropogenic NMVOCs emission inventories in China, *Atmos. Chem. Phys.,* 8, 7297-7316, 2008.

China State Council: Twelfth Five-Year Plan on National Economy and Social Development of the People's Republic of China, 2011. http://www.gov.cn/2011lh/content_1825838.htm (in Chinese).

Cooper, O. R., Gao, R.-S., Tarasick, D., Leblanc, T., and Sweeney, C.: Long-term ozone trends at rural

25   ozone monitoring sites across the United States, 1990–2010, *J. Geophys. Res. –Atmos.,* 117, D22307, doi: 10.1029/2012jd018261, 2012.

Cooper, O. R., Parrish, D. D., Ziemke, J., Balashov, N. V., Cupeiro, M., Galbally, I. E., Gilge, S., Horowitz, L., Jensen, N. R., Naik, V., Oltmans, S. J., Schwab, J., Shindell, D. T., Thompson, A. M.,

Thouret, V., Wang, Y., and Zbinden, R. M.: Global distribution and trends of tropospheric ozone: An observation-based review, *Elementa Sci. of Anth.,* 2, 000029, 2014.

Crutzen, P.: A discussion ofthe chemistry of some minor constituents in the stratosphere and troposphere, *Pure Appl. Geophys.,* 106-108, 1385-1399, 1973.

5   Ding, A. J., Wang, T., Thouret, V., Cammas, J.-P., and Nédélec, P.: Tropospheric ozone climatology over Beijing: analysis of aircraft data from the MOZAIC program, *Atmos. Chem. Phys.,* 8, 1-13, 2008.

Ding, A. J., Fu, C. B., Yang, X. Q., Sun, J. N., Zheng, L. F., Xie, Y. N., Herrmann, E., Nie, W., Petaja, T., Kerminen, V.-M., and Kulmala, M.: Ozone and fine particle in the western Yangtze River Delta: an overview of 1 yr data at the SORPES station, *Atmos. Chem. Phys.,* 13, 5813-5830, 2013.

10   Draxler, R. R., Stunder, B., Rolph, G., and Taylor, A.: HYSPLIT4 user's guide, http://ready.arl.noaa.gov/HYSPLIT_info.php, 2009.

Gao, J., Wang, T., Ding, A. J., and Liu, C. B.: Observational study of ozone and carbon monoxide at the summit of mount Tai (1534m asl) in central-eastern China, *Atmos. Environ.,* 39, 4779-4791, 2005.

Guo, J., Wang, Y., Shen, X., Wang, Z., Lee, T., Wang, X., Li, P., Sun, M., Collett Jr, J. L., Wang, W., and Wang, T.: Characterization of cloud water chemistry at Mount Tai, China: Seasonal variation, anthropogenic impact, and cloud processing, *Atmos. Environ.,* 60, 467-476, 2012.

IPCC: Climate Change: The Assessment Reports of the Intergovernmental Pane on Climate Change, Cambridge University Press, Cambridge, UK, 2013.

Kanaya, Y., Akimoto, H., Wang, Z. F., Pochanart, P., Kawamura, K., Liu, Y., Li, J., Komazaki, Y., Irie, H., and Pan, X. L., Taketani, F., Yamaji, K., Tanimoto, H., Inomata, S., Kato, S., Suthawaree, J., Okuzawa, K., Wang, G., Aggarwal, S. G., Fu, P. Q., Wang, T., Gao, J., Wang, Y., and Zhuang, G. S.: Overview of the Mount Tai Experiment (MTX2006) in central East China in June 2006: studies of significant regional air pollution, *Atmos. Chem. Phys.,* 13, 8265-8283, 2013.

Lee, H.-J., Kim, S.-W., Brioude, J., Cooper, O. R., Frost, G. J., Kim, C.-H., Park, R. J., Trainer, M., and Woo, J.-H.: Transport of NO_x in East Asia identified by satellite and in situ measurements and Lagrangian particle dispersion model simulations, *J. Geophys. Res. Atmos.,* 119, 2574-2596, 2013.

Lefohn, A. S., Shadwick, D., and Oltmans, S. J.: Characterizing changes in surface ozone levels in metropolitan and rural areas in the United States for 1980–2008 and 1994–2008, *Atmos. Environ.,* 44, 5199-5210, 2010.

30   Lin, M., Holloway, T., Oki, T., Streets, D. G., and Richter, A.: Multi-scale model analysis of boundary layer ozone over East Asia, *Atmos. Chem. Phys.,* 9, 3277-3301, 2009.

Lin, M., Horowitz, L. W., Oltmans, S. J., Fiore, A. M., and Fan, S.: Tropospheric ozone trends at Mauna Loa Observatory tied to decadal climate variability, *Nature Geosci.,* 7, 136-143, 2014.

Lin, W., Xu, X., Zhang, X., and Tang, J.: Contributions of pollutants from North China Plain to surface ozone at the Shangdianzi GAW Station, *Atmos. Chem. Phys.,* 8, 5889-5898, 2008.

5   Lin, Y.-K., Lin, T.-H., and Chang, S.-C.: The changes in different ozone metrics and their implications following precursor reductions over northern Taiwan from 1994 to 2007, *Environ. Monit. Assess.,* 169, 143-157, 2010.

Logan, J. A., Staehelin, J., Megretskaia, I. A., Cammas, J.-P., Thouret, V., Claude, H., De Backer, H., Steinbacher, M., Scheel, H.-E., Stübi, R., Fröhlich, M., and Derwent, R.: Changes in ozone over

10   Europe: Analysis of ozone measurements from sondes, regular aircraft (MOZAIC) and alpine surface sites, *J. Geophys. Res.-Atmos.,* 117, D09301, doi: 10.1029/2011jd016952, 2012.

Lu, Z., Streets, D. G., Zhang, Q., Wang, S., Carmichael, G. R., Cheng, Y. F., Wei, C., Chin, M., Diehl, T., and Tan, Q.: Sulfur dioxide emissions in China and sulfur trends in East Asia since 2000, *Atmos. Chem. Phys.,* 10, 6311-6331, 2010.

15   Ma, J., Zhou, X., and Hauglustaine, D.: Summertime tropospheric ozone over China simulated with a regional chemical transport model 2. Source contributions and budget, *J. Geophys. Res.-Atmos.,* 107 (D22), 4612, doi:10.1029/2001jd001355, 2002.

Mao, H., and Talbot, R.: Role of meteorological processes in two New England ozone episodes during summer 2001, *J. Geophys. Res.,* 109, D20305, doi:10.1029/2004jd004850, 2004.

20   Monks, P. S., Archibald, A., Colette, A., Cooper, O., Coyle, M., Derwent, R., Fowler, D., Granier, C., Law, K. S., Mills, G. E., Stevenson, D. S., Tarasova, O., Thouret, V., von Schneidemesser, E., Sommariva, R., Wild, O., and Williams, M. L.: Tropospheric ozone and its precursors from the urban to the global scale from air quality to short-lived climate forcer, *Atmos. Chem. Phys.,* 15, 8889-8973, 2015.

25   National Research Council: Rethinking the Ozone Problem in Urban and Regional Air Pollution, *Natl. Acad. Press,* Washington, D. C., 1991.

Ohara, T., Akimoto, H., Kurokawa, J.-I., Horii, N., Yamaji, K., Yan, X., and Hayasaka, T.: An Asian emission inventory of anthropogenic emission sources for the period 1980–2020, *Atmos. Chem. Phys.,* 7, 4419-4444, 2007.

30   Oltmans, S. J., Lefohn, A. S., Shadwick, D., Harris, J. M., Scheel, H. E., Galbally, I., Tarasick, D. W., Johnson, B. J., Brunke, E.-G., Claude, H., Zeng, G., Nichol, S., Schmidlin, F., Davies, J., Cuevas, E., Redondas, A., Naoe, H., Nakano, T., and Kawasato, T.: Recent tropospheric ozone changes - A pattern dominated by slow or no growth, *Atmos. Environ.,* 67, 331-351, 2013.

Parrish, D. D., Law, K. S., Staehelin, J., Derwent, R., Cooper, O. R., Tanimoto, H., Volz-Thomas, A., Gilge, S., Scheel, H. E., Steinbacher, M., and Chan, E.: Long-term changes in lower tropospheric baseline ozone concentrations at northern mid-latitudes, *Atmos. Chem. Phys.,* 12, 11485-11504, 2012.

Parrish, D. D., Lamarque, J. F., Naik, V., Horowitz, L., Shindell, D. T., Staehelin, J., Derwent, R.,
5   Cooper, O., Tanimoto, H., Volz-Thomas, A., Gilge, S., Scheel, H.-E., Steinbacher, M., and Chan, E.: Long-term changes in lower tropospheric baseline ozone concentrations: Comparing chemistry-climate models and observations at northern midlatitudes, *J. Geophys. Res.-Atmos.,* 119, 5719-5736, doi:10.1002/2013jd021435, 2014.

Seinfeld, J. H., and Pandis, S. N.: Atmospheric Chemistry and Physics: From Air Pollution to Climate
10   Change., Wiley, 2006.

Seo, J., Youn, D., Kim, J., and Lee, H.: Extensive spatiotemporal analyses of surface ozone and related meteorological variables in South Korea for the period 1999–2010, *Atmos. Chem. Phys.,* 14, 6395-6415, 2014.

Shen, X., Lee, T., Guo, J., Wang, X., Li, P., Xu, P., Wang, Y., Ren, Y., Wang, W., Wang, T., Li, Y.,
15   Carn, S. A., and Collett Jr, J. L.: Aqueous phase sulfate production in clouds in eastern China, *Atmos. Environ.,* 62, 502-511, 2012.

Shindell, D., Kuylenstierna, J. C., Vignati, E., van Dingenen, R., Amann, M., Klimont, Z., Anenberg, S. C., Muller, N., Janssens-Maenhout, G., Raes, F., Schwartz, J., Faluvegi, G., Pozzoli, L., Kupianinen, K., H-Isaksson, L., Emberson, L., Streets, D., Ramanathan, V., Hicks, K., Oanh, N. T., Milly, G.,
20   Williams, M., Demkine, V., and Fowler, D.: Simultaneously mitigating near-term climate change and improving human health and food security, *Science*, 335, 183-189, 2012

Stevenson, D. S., Young, P. J., Naik, V., Lamarque, J.-F., Shindell, D. T., Voulgarakis, A., Skeie, R., Dalsoren, S. B., Myhre, G., Berntsen, T. K., Folberth, G. A., Rumbold, S. T., Collins, W. J., Mackenzie, I. A., Doherty, R. M., Zeng, G., van Noijie, T. P. C., Strunk, A., Bergmann, D.,
25   Cameron-Smith, P., Plummer, D. A., Strode, S. A., Horowitz, L., Lee, Y. H., Szopa, S., Sudo, K., Nagashima, T., Josse, B., Cionni, I., Righi, M., Eyring, V., Conley, A., Bowman, K. W., Wild, O., and Archibald, A.: Tropospheric ozone changes, radiative forcing and attribution to emissions in the Atmospheric Chemistry and Climate Model Intercomparison Project (ACCMIP), *Atmos. Chem. Phys.,* 13, 3063-3085, 2013.

30   Stohl, A., Bonasoni, P., Cristofanelli, P., Collins, W. J., Feichter, J., Frank, A., Forster, C., Gerasopoulos, E., Gäggeler, H., James, P., Kentarchos, T., Kromp-Kalb, H., Kruger, B., Land, C., Meloen, J., Papayannis, A., Priller, A., Seibert, P., Sprenger, M., Roelofs, G. J., Scheel, H. E., Schnabel, C., Siegmund, P., Tobler, L., Trickl, T., Wernli, H., Wirth, V., Zanis, P., and Zerefos, C.:

Atmospheric
Chemistry
and Physics
Discussions

Stratosphere-troposphere exchange: A review, and what we have learned from STACCATO, *J. Geophys. Res.-Atmos.,* 108, 8516, doi:10.1029/2002jd002490, 2003.

Suthawaree, J., Kato, S., Okuzawa, K., Kanaya, Y., Pochanart, P., Akimoto, H., Wang, Z., and Kajii, Y.: Measurements of volatile organic compounds in the middle of Central East China during Mount Tai Experiment 2006 (MTX2006): observation of regional background and impact of biomass burning, *Atmos. Chem. Phys.,* 10, 1269-1285, 2010.

Tang, G., Li, X., Wang, Y., Xin, J., and Ren, X.: Surface ozone trend details and interpretations in Beijing, 2001–2006, *Atmos. Chem. Phys.,* 9, 8813-8823, 2009.

The Royal Society: Ground-level Ozone in the 21st century: Future Trends, Impacts and Policy Implications, Royal Society policy document 15/08, RS1276, 2008. Available at http://royalsociety.org/Report_WF.aspx?pageid57924&terms5groundlevel1ozone

Trainer, M., Parrish, D. D., Buhr, M. P., Norton, R. B., Fehsenfeld, F. C., Anlauf, K. G., Bottenheim, J. W., Tang, Y. Z., Wiebe, H. A., Roberts, J. M., Tanner, R. L., Newman, L., Bowersox, V. C., Meagher, J. F., Olszyna, K. J., Rodgers, M. O., Wang, T., Berresheim, H., Demerjian, K. L., Roychowdhury, U. K.: Correlation of ozone with NO_y in photochemically aged air, *J. Geophys. Res.-Atmos.,* 98 (D2), 2917-2925, doi:10.1029/92jd01910, 1993.

UNEP and WMO: Integrated Assessment of black carbon and tropospheric ozone: Summary for decision makers, United Nations Environment Programme, Nairobi, Kenya, 2011.

Wang, S. X., Zhao, B., Cai, S., Klimont, Z., Nielsen, C. P., Morikawa, T., Woo, J. H., Kim, Y., Fu, X., Xu, J. Y., Hao, J. M., and He, K. B.: Emission trends and mitigation options for air pollutants in East Asia, *Atmos. Chem. Phys.,* 14, 6571-6603, 2014.

Wang, T., Wei, X. L., Ding, A. J., Poon, C. N., Lam, K. S. , Li, Y. S., Chan, L. Y., and Anson, M.: Increasing surface ozone concentrations in the background atmosphere of Southern China, 1994–2007, *Atmos. Chem. Phys.,* 9, 6217-6227, 2009.

Wang, T., Nie, W., Gao, J., Xue, L. K., Gao, X. M., Wang, X. F., Qiu, J., Poon, C. N., Meinardi, S., Blake, D. R., Wang, S. L., Ding, A. J., Chai, F. H., Zhang. Q. Z., and Wang. W. X.: Air quality during the 2008 Beijing Olympics: secondary pollutants and regional impact, *Atmos. Chem. Phys.,* 10, 7603-7615, 2010.

Xu, W. Y., Lin, W. L., Xu, X. B., Tang, J., Huang, J. Q., Wu, H., and Zhang, X. C.: Long-term trends of surface ozone and its influencing factors at the Mt. Waliguan GAW station, China – Part 1: Overall trends and characteristics, *Atmos. Chem. Phys. Discuss.,* 15, 30987-31024, 2015.

Atmospheric
Chemistry
and Physics
Discussions

Open Access

EGU

Xu, X., Lin, W., Wang, T., Yan, P., Tang, J., Meng, Z., and Wang, Y.: Long-term trend of surface ozone at a regional background station in eastern China 1991–2006: enhanced variability, *Atmos. Chem. Phys.*, 8, 2595-2607, 2008.

Xu, Z., Wang, T., Xue, L. K., Louie, P. K. K., Luk, C. W. Y., Gao, J., Wang, S. L., Chai, F. H., and Wang, W. X.: Evaluating the uncertainties of thermal catalytic conversion in measuring atmospheric nitrogen dioxide at four differently polluted sites in China, *Atmos. Environ.*, 76, 221-226, 2013.

Xue, L. K., Wang, T., Zhang, J. M., Zhang, X. C., Deligeer, Poon, C. N., Ding, A. J., Zhou, X. H., Wu, W. S., Tang, J., Zhang, Q. Z., and Wang, W. X.: Source of surface ozone and reactive nitrogen speciation at Mount Waliguan in western China: New insights from the 2006 summer study, *J. Geophys. Res.-Atmos.*, 116 (D7), D07306, doi:10.1029/2010jd014735, 2011.

Xue, L. K., Wang, T., Louie, P. K. K., Luk, C. W. Y., Blake, D. R., and Xu, Z.: Increasing external effects negate local efforts to control ozone air pollution: a case study of Hong Kong and implications for other Chinese cities, *Environ. Sci. Tech.*, 48, 10769-10775, 2014.

Yamaji, K., Li, J., Uno, I., Kanaya, Y., Irie, H., Takigawa, M., Komazaki, Y., Pochanart, P., Liu, Y., Tanimoto, H., Ohara, T., Yan, X., Wang, Z., and Akimoto, H.: Impact of open crop residual burning on air quality over Central Eastern China during the Mount Tai Experiment 2006 (MTX2006), *Atmos. Chem. Phys.*, 10, 7353-7368, 2010.

Zhang, Q., Yuan, B., Shao, M., Wang, X., Lu, S., Lu, K., Wang, M., Chen, L., Chang, C.-C., and Liu, S.: Variations of ground-level O_3 and its precursors in Beijing in summertime between 2005 and 2011, *Atmos. Chem. Phys.*, 14, 6089-6101, 2014.

Zhang, Y., Ding, A., Mao, H., Nie, W., Zhou, D., Liu, L., Huang, X., Fu, C.: Impact of synoptic weather patterns and inter-decadal climate variability on air quality in the North China Plain during 1980-2013, *Atmos. Envion.*, 124, 119-128, 2016.

Table 1. The observations at Mt. Tai analyzed in the present study.

Year	Month	Observed species	Data source
2003	Jul.-Nov.	O_3, CO	Gao et al. (2005) and our study
2004	Jun.-Aug.	O_3	Kanaya et al.(2013)[a]
2005	Jun.-Aug.	O_3	Kanaya et al.(2013)[a]
2006	Jun.-Dec.	O_3, NO_2*, NO	Our study
2007	Mar.-Dec.	O_3, NO, NO_2*, CO	Our study [b]
2008	Jan.-Dec.	O_3, NO, NO_2*, CO	Our study
2009	Jan.-Jun.	O_3, NO, NO_2*, CO	Our study
2014	Jun.-Aug.	O_3, NO_x*, CO	Our study [c]
2015	Jun.-Aug.	O_3, NO, NO_2*, CO	Our study [c]

[a] Monthly average data were taken from Kanaya et al. (2013).

[b] Valid NO and NO_2* data were only available in March-April and July-December, and CO was available in March-April in 2007.

5 [c] Note that the intensive measurement periods were 6 June – 3 July & 24 July – 26 August in 2014 and 14 June – 8 August in 2015.

Atmospheric
Chemistry
and Physics

Open Access

EGU

Discussions

Table 2. Summary of meteorological conditions recorded at Mt. Tai in June and July-August over 2003-2015[a].

Year	June			July-August		
	Temperature (℃)	RH (%)	Prevailing WD	Temperature (℃)	RH (%)	Prevailing WD
2003	15.4±3.1	70.9±19.2	SW	17.3±2.9	88.3±16.3	SW
2004	15.4±3.9	74.4±21.2	SW	17.0±2.5	86.8±15.5	SSW
2005	18.1±3.2	65.0±22.0	SSW	17.4±2.9	86.8±16.3	SW
2006	17.2±2.9	67.8±21.4	SSW	18.3±2.0	88.3±16.3	SSW
2007	17.0±2.8	71.4±27.3	E	17.8±2.3	85.2±21.1	E
2008	15.0±3.6	76.9±20.0	S	17.0±2.3	86.3±14.6	S
2009	17.9±3.1	57.8±22.2	SSW	17.4±2.9	78.7±21.8	S
2010	15.9±3.6	80.1±18.7	SW	18.2±2.7	91.0±16.9	SW
2011	16.6±2.7	72.6±21.1	SSW	17.6±2.5	87.6±16.1	S
2012	16.8±3.2	71.0±23.8	SW	18.2±2.4	89.5±17.9	E
2013	16.1±3.1	79.8±19.6	SW	19.3±2.4	88.2±15.6	SW
2014	15.3±2.9	79.9±17.6	SW	16.5±2.3	86.7±14.6	SW
2015	15.8±2.8	70.5±21.0	SW	18.0±2.1	86.1±16.9	SW

[a] Average and standard deviations are provided.

Table 3. Statistics of O_3, NO_2* and CO in different air mass categories [a]

June				July-August			
Air mass [b]	O_3	NO_2*	CO	Air mass [b]	O_3	NO_2*	CO
M&EC	92±27	7.2±5.3	500±300	M&EC	64±22	3.6±2.9	370±180
CC	89±24	6.3±5.0	550±300	CC	77±21	3.3±2.5	440±180
NEC	94±25	7.0±4.5	380±180	NEC	73±22	4.5±4.2	380±180
M&NC	78±21	4.0±3.3	280±180	SEC	58±17	4.1±2.4	350±80

5   [a] The unit is ppbv; average and standard deviations are provided.

[b] Refer to *Figure* 5 and Section 3.2 for the derivation and description of the air mass types.

Atmospheric
Chemistry
and Physics
Discussions

Table 4. Summary of surface and lower tropospheric ozone trends recorded in East Asia.

| Station	Site type	Period	Rate of change (ppbv yr^{-1})	Reference
Mt. Tai	rural	2003-2015 (summer)	1.7 ± 1.0 (June) 2.1 ± 0.9 (July-August)	This study
Beijing	rural (MOZAIC)	1995-2005	~1 (annual average)	Ding et al. (2008)
Hong Kong (Hok Tsui)	rural	1994-2007	~3 (summer afternoon) 0.58	Wang et al. (2009)
Hong Kong	urban & suburban	2002-2013 (autumn)	0.54 ± 0.49	Xue et al. (2014)
Lin'an	rural	1991-2006	2.7% (summer daily maximum)	Xu et al. (2008)
Waliguan	remote	1994-2013 (summer)	0.15 ± 0.19	Xu et al. (2015)
Taiwan (Yangming)	rural	1994-2007	0.54 ± 0.21	Lin et al. (2010)
Mt. Happo, Japan	rural	1991-2011 (summer)	0.64 ± 0.40	Parrish et al. (2012)
Tokyo, Japan	urban & suburban	1990-2010	0.31 ± 0.02	Akimoto et al. (2015)
Nagoya, Japan	urban & suburban	1990-2010	0.22 ± 0.05	Akimoto et al. (2015)
Osaka/Kyoto, Japan	urban & suburban	1990-2010	0.37 ± 0.03	Akimoto et al. (2015)
Fukuoka, Japan	urban & suburban	1990-2010	0.37 ± 0.04	Akimoto et al. (2015)
South Korea	124 urban sites average	1999-2010	0.26	Seo et al. (2014)
South Korea	56 urban sites average	1990-2010	0.48 ± 0.07 (annual average) 0.55 ± 0.13 (summer)	Lee et al. (2013)
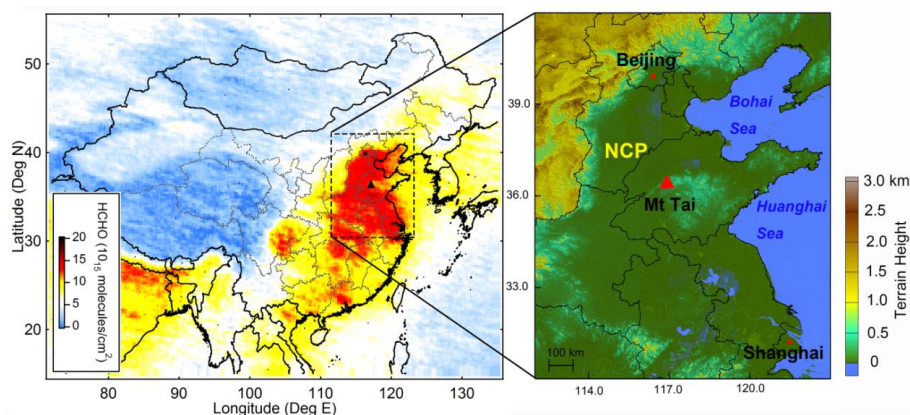
Figure 1. Geographical map showing the North China Plain and the location of Mt. Tai. The left map is color-coded by the HCHO column density in the summer period (JJA; 2003–2014) retrieved from SCIAMACHY and GOME-2(B).
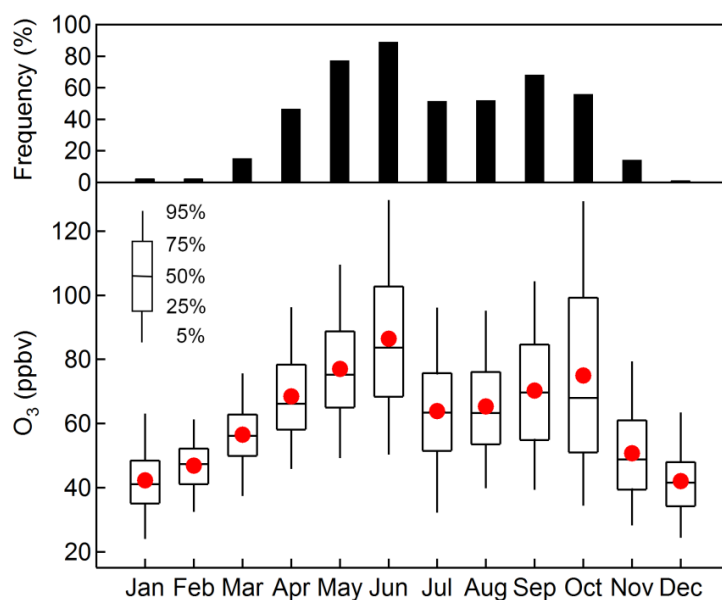

Figure 2. Seasonal variation of surface O_3 mixing ratios at Mt. Tai derived from the continuous observations from 2006–2009. Red dots indicate the monthly average O_3 concentrations. Shown in the upper panel is the frequency of the MDA8 O_3 exceeding the Chinese national ambient air quality standard, i.e. 75 ppbv (Class II).

23
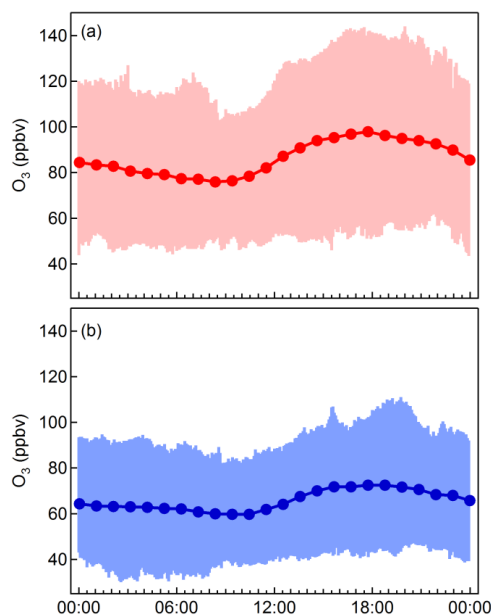
Figure 3. Average diurnal variations of surface O_3 at Mt. Tai in (a) June and (b) July-August derived from the continuous observations from 2006–2009. The shaded area indicates the 5th and 95th percentiles of the data.
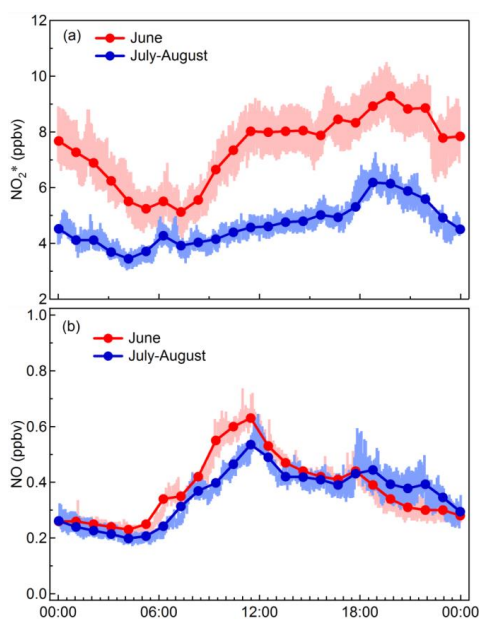
Figure 4. Average diurnal variations of (a) NO_2^* and (b) NO at Mt. Tai in June and July-August derived from the continuous observations from 2006–2009. The shaded area indicates the standard error of the mean.
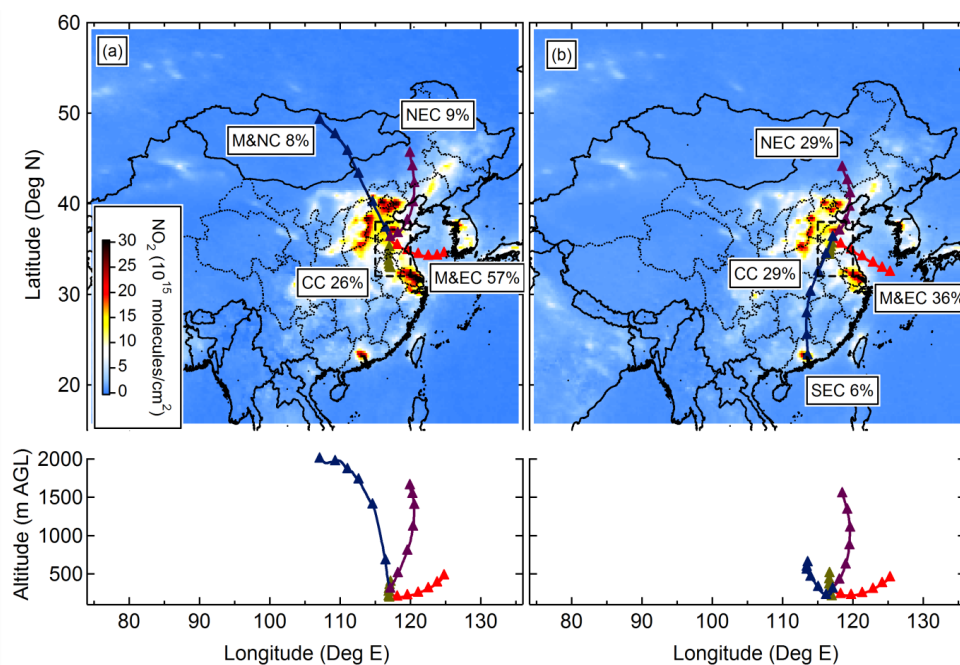
Atmospheric
Chemistry
and Physics

Discussions

Open Access

Figure 5. Climatological air mass transport pattern at Mt. Tai in (a) June and (b) July-August over 2003-2015. The maps are color-coded by the NO_2 column density retrieved from SCIAMACHY (2003-2011) and GOME-2 (B) (2013-2015). The box (dashed line) refers to the domain for which the satellite retrievals were averaged. Five major air masses: (1) M&EC: Marine and East China, (2) NEC: Northeast China, (3) CC: Central China, (4) SEC: Southeast China, (5) M&NC: Mongolia and North China.
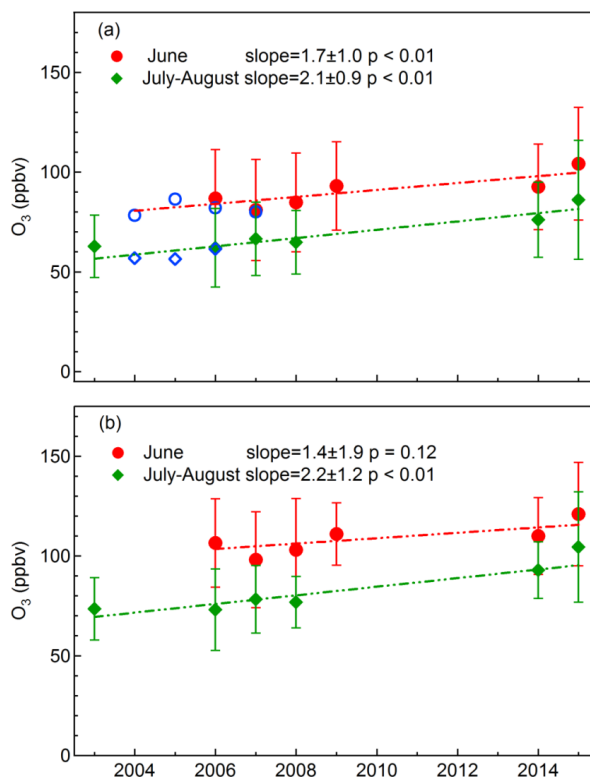
Figure 6. Monthly averaged (a) 1-hour and (b) MDA8 O_3 mixing ratios at Mt. Tai in June and July-August over 2003-2015. Error bars indicate the standard deviation of the mean. The blue open circles and squares represent the data taken from Kanaya et al. (2013). The fitted lines are derived from the least square linear regression analysis with the slopes ($\pm$ 95% confidence intervals) and p values annotated.
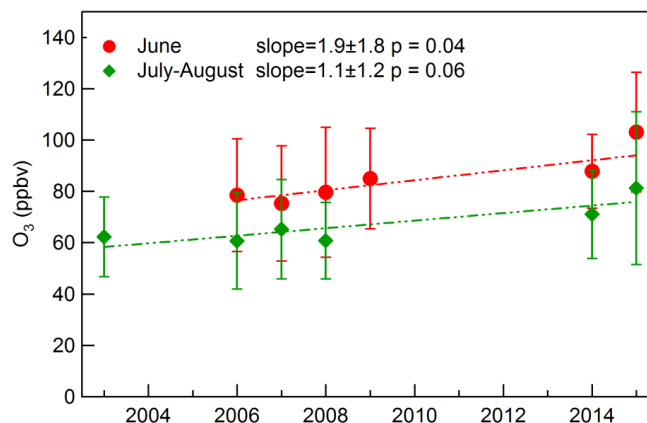

Figure 7. Monthly averaged nighttime O_3 mixing ratios (inferring the regional background O_3) at Mt. Tai in June and July-August over 2003-2015. Error bars indicate the standard deviation of the mean. The fitted lines are derived from the least square linear regression analysis with the slopes ($\pm$ 95% confidence intervals) and p values annotated.

Atmospheric
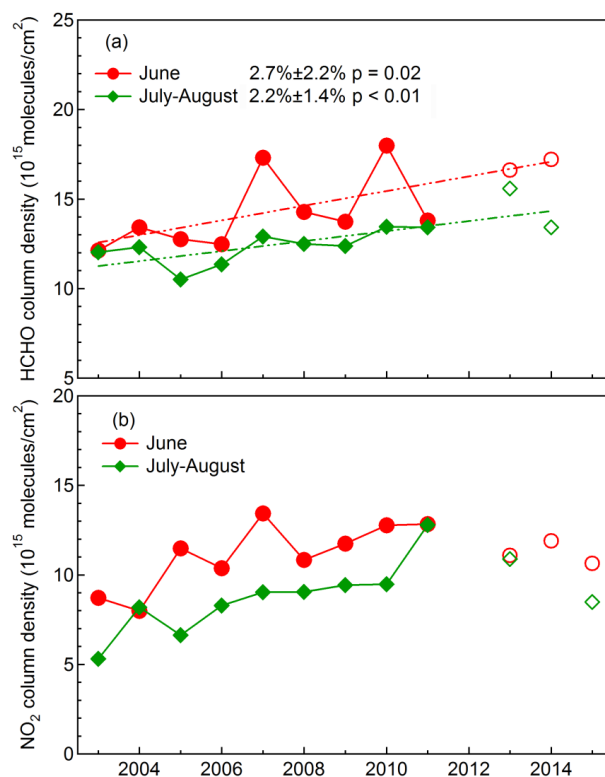Chemistry
and Physics
Discussions

Figure 8. Monthly average column density of (a) formaldehyde and (b) NO₂ retrieved from SCIAMACHY (2003–2011; solid markers) and GOME-2 (B) (2013–2015; open markers) for the target domain (32 °–38 °N,115 °–120 °E). For formaldehyde, the fitted lines are derived from the least square linear regression analysis with the slopes (±95% confidence intervals) and p values also shown.

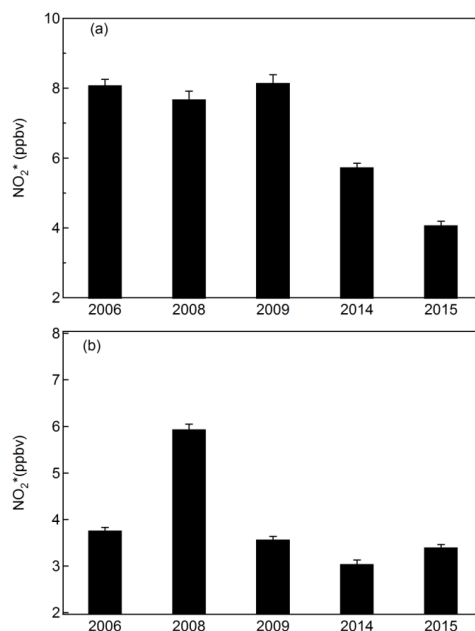Atmospheric
Chemistry
and Physics
Discussions

Figure 9. Monthly averaged NO$_2$* concentrations measured at Mt. Tai in (a) June and (b) July-August during 2006–2015. Error bars indicate the standard error of the mean. Note that the data point in June 2014 is for NOx* instead of NO$_2$*.
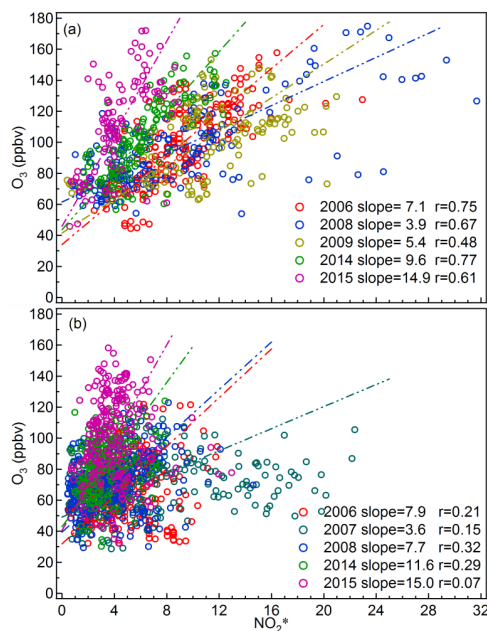

Figure 10. Scatter plots of O$_3$ versus NO$_2$* at Mt. Tai in (a) June and (b) July–August during 2006–2015. Only the afternoon data (i.e., 12:00-18:00 local time) were used for this analysis. Note that the NO$_2$* data in June 2014 stand for NOx* (NO$_x$*=NO+NO$_2$*), of which NO usually presents a minor fraction. The slopes are determined by the reduced major axis (RMA) method.